ABSOLUTE PHOTOFISSION CROSS SECTION OF ^{197}Au, ^{nat}Pb, ^{209}Bi, ^{232}Th, ^{238}U and ^{235}U NUCLEI BY 69-MEV MONOCHROMATIC AND POLARIZED PHOTONS

by

J.B. MARTINS[1], E.L. MOREIRA[1], O.A.P. TAVARES[1], J.L. VIEIRA[1],
L. CASANO[2], A. D'ANGELO[2], C. SCHAERF[2], M.L. TERRANOVA[3],
D. BABUSCI[4] and B. GIROLAMI[5]

[1]Centro Brasileiro de Pesquisas Físicas - CBPF/CNPq
Rua Dr. Xavier Sigaud, 150
22290 - Rio de Janeiro, RJ - Brasil

[2]Dipartimento di Fisica, II Università degli Studi di Roma
"Tor Vergata", Via E. Carnevale, 00173 Roma, Italy.
Istituto Nazionale di Fisica Nucleare-INFN, Sezione di Roma 2, Roma, Italy.

[3]Dipartimento di Scienze e Tecnologie Chimiche, II Università degli Studi
di Roma "Tor Vergata", Via E. Carnevale, 00173 Roma, Italy
Istituto Nazionale di Fisica Nucleare-INFN, Sezione di Roma 2, Roma, Italy.

[4]Istituto Nazionale di Fisica Nucleare-INFN, Laboratori Nazionali
di Frascati-LNF, Casella Postale 13,00044 Frascati, Italy.

[5]Laboratorio di Fisica dell'Istituto Superiore di Sanità,
Viale Regina Elena 299, 00161 Roma, Italy.
Istituto Nazionale di Fisica Nucleare-INFN, Sezione Sanità,
Roma, Italy

ABSTRACT - Absolute cross section measurements for the photofission reactions of ^{197}Au, ^{nat}Pb, ^{209}Bi, ^{232}Th, ^{238}U, and ^{235}U nuclei have been performed at an incident photon energy of 69 MeV using the monochromatic and polarized LADON photon beams and dielectric fission-track detectors. Nuclear fissility values have been obtained and results are in agreement with those from other laboratories, although in some cases discrepancies are observed between one other. For nuclei in the region of the actinides the fissility resulted to be ≥ 0.4, while for Au, Pb and Bi nuclei it amounts to $\sim 10^{-3}$-10^{-2} only. Results have been interpreted in terms of the primary Levinger's quasi-deuteron nuclear photoabsorption followed by a mechanism of evaporation-fission competition for the excited nuclei. Shell effects have been taken into account, and they are clearly manifested when fissility is evaluated. The influence of photon polarization on photofission of ^{238}U has been also investigated, and results have shown isotropy in the fragment azimuthal distribution.

Key-words: Fission reactions; Photofission.

1. - Introduction.

In recent years, the development of new techniques which led to the production of high-quality monochromatic (or quasi-monochromatic) photon beams of energies above ~ 20 MeV or so has given the opportunity of obtaining reliable photonuclear cross section data[1-16]. Attention has been particularly concentrated on photofission reactions of nuclei of mass number A $\gtrsim$ 200 for both quasi-deuteron (~ 30-140 MeV)[1,6,11,13,14,16] and photomesonic ($\gtrsim$ 140 MeV)[3,5,10,12,15] regions of primary photon-nucleus interaction, and the current photonuclear reaction models are being refined to give a deeper insight about the mechanisms of photofission at these energies[10,11,15,17-19]. Photofission cross section data have also been obtained from threshold on by unfolding the electrofission yields with a virtual photon spectrum[20-22].

As far as the incident photon energy range ~ 30-120 MeV is concerned, most photofission data have indicated fissility values near 1 for target nuclei in the region of actinides, and about 10^{-3}-10^{-2} for nuclei of 200 $\lesssim$ A $\leq$ 210. Experimental results have been discussed in terms of a primary photoabsorption via n-p pairs (Levinger's quasi-deuteron photoabsorption model[23]) followed by a fission-evaporation competition model for the excited residual nucleus[24,25], leading to good agreement between experimental and calculated fissility values.

The photofission studies mentioned above have discussed the dependence of cross section and fissility on incident photon energy or excitation energy, for a given target nucleus. Since at moderate excitation energies nuclear shell effects are not completely destroyed, we thought it important to investigate such effects by collecting a number of photofission data obtained at the same energy, but different target nuclei, including of course some nuclei located near ^{208}Pb.

Recently we have used the LADON facility of the Frascati National Laboratories (INFN-LNF, Frascati, Italia) as a source of photons (monochromatic, polarized and intense) in the energy range 30-80 MeV to measure absolute photofission cross section and fissility of ^{238}U and of nuclei of relatively low fission barriers[13,14]. In the present work we report new data obtained at a constant effective photon mean energy of 69 MeV for a set of six target nuclei (^{197}Au, ^{nat}Pb, ^{209}Bi, ^{232}Th, ^{238}U and ^{235}U). Results are compared with those from other laboratories as well as with fissility values calculated from a simplified description of the photofission reactions, in which the influence of shell effects on fissility can be examined. In the case of ^{238}U nucleus we also investigated the effect of photon polarization on the azimuthal distribution of fission fragments.

2. - Experimental Procedure.

2.1. - Targets and Detectors. - The target materials used in the experiment consisted of metal films of high-purity natural gold ($\sim$ 1.4 mg/cm^2), lead ($\sim$ 4.1 mg/cm^2), and bismuth ($\sim$ 5.7 mg/cm^2) prepared by vacuum evaporation on $\sim$ 3.5 cm x 3.5 cm thin foils (1.72 mg/cm^2 thick) of mylar as supports, and thin films of natural thorium, natural uranium, and 93%-enriched ^{235}U oxides produced by the "parlodion ignition" method[26] on $\sim$ 4 cm x 4 cm sheets of muscovite mica ($\sim$ 25 mg/cm^2 thick) which served as supports and/or detectors for fission fragments. The clean, freshly cleaved micas were selected and pre-etched in 49% hydrofluoric acid during $\sim$ 5 h at room temperature to produce large diamond-shaped pits of fossil fission tracks so as to distinguish them later from photon-induced fission tracks. The parlodion ignition method gives quite uniform extra-thin films of UO$_3$ and ThO$_2$ of typical thickness of 0.21-0.30 mg/cm^2. In all cases the target thicknesses were determined by mass measurements.

The Au, Pb, Bi, and ^{238}U target samples were placed in intimate contact with sheets of 100μm—thick makrofol N (Bayer AG) used as fission track detectors, and pairs of micas containing the ^{235}UO$_3$ or ^{232}ThO$_2$ films were contacted so as to form sandwiches of these oxides. The target-detector systems were arranged in stacks, enveloped between two sheets of a heat-sealable plastics, and then vacuum

packed. The contents of the target-detector stacks are shown in Table I.

2.2. - Irradiation. - The packs containing the target-detector materials were exposed to monochromatic ($\sim$ 9% FWHM of energy resolution) and fully polarized photon beams of maximum photon energy of 78.8 MeV produced in the LADON facility of the Frascati National Laboratories, as a result of the scattering of laser light by the high-energy electrons circulating in the storage ring ADONE (Compton backscattering[27-29]). The experimental layout is shown schematically in Fig. 1, and the irradiation conditions are listed in Table I. The integral photon doses were measured by a 10-in x 10-in NaI(Tl) crystal monitor (threshold energy $\sim$ 9 MeV), and its threshold stability was periodically controlled. Besides, the energy spectra of the photon beams were continuously taken by a magnetic pair spectrometer. The spectra did not indicate significant deviations from the mean energy profile (typical energy spectra are shown in Fig. 2). Finally, the background due to continuous bremsstrahlung (integrated over the entire energy range) was estimated to less than 5% by switching off the laser light.

2.3. - Detector processing and scanning. - After irradiations, the detectors were processed by the usual

etching procedures to obtain visible fission tracks for track counting and measurement by conventional optical microscopy. The mica sheets used as detectors were first immersed in a dilute ($\sim$ 20%) nitric acid solution at 40°C during $\sim$ 1 h to remove completely the uranium- and thorium-oxide layers. Since measurements of azimuthal angle require good definition of fission-track direction, it was necessary to search for best conditions of track etching to be applied in the case of ^{238}U target. By exposing a number of makrofol sheets in 2π-geometry to fission fragments from a laboratory ^{252}Cf-source, and by varying the etching conditions of NaOH solutions, it was possible to decide about the conditions of track revelation appropriate to angle measurements. The etching procedures used for the different detectors are given in Table II.

The scanning of the detectors and the analysis of the etched fission tracks were carried out by using Leitz Ortholux microscopes. Since the expected fission-track population was low, track counting and track identification on each detector were done by two observers and checked by a third one. From the mapping of the recorded events, and by applying the statistical method of double scan[30], the true number of fission tracks and counting efficiency as well were determined. Table II lists some data regarding the scanning work.

3. - Data analysis and results.

To obtain the final values of the physical quantities of interest and associated errors, the data have been treated taking into account the geometry of irradiation, statistics of track counting and efficiency, registration efficiency, energy absorption effects of fission fragments by thick target samples (Au, Pb and Bi), and background. This latter consisted of fission tracks originated essentially from spontaneous fission of ^{238}U and neutron-induced fission of ^{235}U (the time elapsed between sample preparation and processing allowed the detection of small ^{238}U impurities in the Th and Pb samples). In addition, since the actinide targets exhibit a resonant pattern in the photofission cross section curve at energies below ~ 30MeV, the fraction of the fission events that might be induced by the continuous bremsstrahlung background was considered for such target nuclei (see section 3.2).

3.1. - Beam polarization effect on ^{238}U fission. - From direct measurements of the azimuthal angle (within ± 3°) over 2370 fission tracks recorded, the fragment azimuthal angle distribution for ^{238}U fission was obtained (Fig. 3). The relative large number of spontaneous fission tracks served to construct a standard distribution, and so to check the quality of the track recording method. By subtracting these tracks from the distribution of the total recorded tracks, one obtained the distribution for the photon-induced

fission tracks (bottom of Fig. 3). As it is seen, no polarization effect was detected under the conditions of the present experiment. This result may be due to the fact that fission takes place in a time which is distant from the moment of photon primary interaction, in such a way that the excited fissioning nucleus lost the memory of the physical details of the primary photon absorption.

3.2. - Photofission yield. - In photon-induced reactions, the fission yield measured, $Y(k_{max})$, represents the sum of the contributions to the total number of fission events N_f, due to all incident photons, Q, of the energy distribution of photon maximum energy k_{max}. This is expressed by the relationship

$$Y(k_{max}) = \frac{N_f}{Q\ N_a} = \int_{k_{th}}^{k_{max}} \sigma(k)n(k,k_{max})dk, \qquad (1)$$

where N_a is the effective number of target nuclei per unit area, $\sigma(k)$ is the absolute photofission cross section (cross section "per photon") at photon energy k, and $n(k,k_{max})$ is the normalized energy distribution, i.e., $n(k,k_{max})dk$ represents the fraction of photons in the energy interval dk. The photon threshold energy k_{th} is defined in such a way that

$$\int_{0}^{k_{th}} n(k, k_{max}) dk \ll 1. \tag{2}$$

For the energy spectra obtained in the present experiment, it gives $k_{th} \approx 30$ MeV, with $k_{max} = 78.8$ MeV (see Fig. 2).

The contribution to total number of photofission events due to photons of energy $k < k_{th}$ was evaluated to obtain N_f in the range $k_{th}-k_{max}$. This contribution (expressed as fraction, y, of the total number of fissions) comes from fission induced by bremsstrahlung background in the giant resonance region of the actinide targets, and it was estimated by parametrizing the cross section with a Lorentz line, and taking the $1/k$ - energy-distribution actually measured for the bremsstrahlung background spectrum. Next, the net amount of fission events is converted to number of fission tracks recorded, N, by introducing the total efficiency factor, ϵ. Finally, summing over the target-detector pairs forming a stack, the measured photofission yield is obtained by

$$Y = \frac{(1 - y) \ \Sigma_i N_i}{Q \ \overline{\epsilon} \ \Sigma_i N_{a_i}}. \tag{3}$$

The fraction of bremsstrahlung photons in the giant resonance region was evaluated to less than 3%, therefore we

can use Q in (3).

Since in the present experiment we used target samples of different thicknesses (very thin for U and Th, thin for Au, and thick samples for Pb and Bi targets), it was necessary to take into account, for the appropriate corrections to fragment energy, absorption by the target material itself in order to evaluate the effective number of target nuclei and efficiency in each case. This was done by the method described in detail in Ref. 31.

The total uncertainties associated to the photofission yields were estimated by considering both statistical and systematic errors. These latter ones come mainly from uncertainties associated to effective target thickness and efficiency. In order to evaluate the systematic errors for target materials of different thicknesses we considered the basic quantities (and their uncertainties) of the method of measurements of fission yields by the fission-track recording technique[31]: actual thickness of the target sample, minimal track-lenght projection defined by the resolution power of the optical system, thickness of the detector surface removed out during track-etching, and average full residual ranges of fission fragments in both the target and detector media. Systematic errors were estimated to 6% for Th and U targets, 23% for Pb and Bi targets and 30% for Au targets, while the statistical ones amounted to 15% for 235U, 5% for 238U, 9% for 232Th, 22%

for ^{209}Bi, 41% for ^{nat}Pb and 50% for ^{197}Au nuclei.

In addition, a ~ 5% uncertainty in the measurement of the total photon doses was evaluated. The so obtained photofission yields are reported in Table III (last column) where the errors indicated represent a combination of statistical plus systematic errors associated to the quantities related directly to the determination of the yields (columns 2 to 6).

3.3. - Absolute photofission cross section. - The energy spectra of the LADON photon beams could be considered as pure ones, in the sense that the contribution from bremsstrahlung photons to total photon dose was rather small (< 5%). Since for the nuclei under study the dependence of the cross section on photon energy in the range ~ 30-80 MeV can be described to a good approximation by a linear function[10,11,21,22] and the peak shape of the photon energy distributions is reasonably narrow, it follows that $Y \cong \sigma (\overline{k})$, where

$$\overline{k} = \int_{k_{th}}^{k_{max}} k n(k, k_{max}) \, dk \quad . \tag{4}$$

Therefore the measured fission yield gives approximately the absolute fission cross section at photon energy $\overline{k}$. Values of $\overline{k}$ are those reported in Table I (5th

column), and a mean value $\bar{k} = 69$ MeV was assumed as representative value of the photon incident energy for the various energy spectra. Table IV lists in the fourth column the absolute photofission cross section values at 69 MeV of this work as well as those obtained by different authors to allow a comparison.

In the case of ^{235}U, the present result differs from that obtained by Leprêtre et al.[11] by 40%. This difference may be ascribed to difficulties in defining the correct number of photofission tracks, since they were dispersed over an intense background due mainly to neutron-induced fission tracks. For ^{238}U, our result agrees, within the experimental uncertainties, with the interpolated value from data reported by Ivanov et al.[16], although it differs from the measurements by Leprêtre et al.[11] by ~ 33% and from the one reported by Moretto et al.[20] by ~ 57%. Disagreement is noted also when the measurements for ^{232}Th are compared with each other (in this case the difference is of ~ 33%). In the case of ^{209}Bi, however, complete agreement is observed between the measurements of the present experiment and that of ref. 20. The cross-section value by Türck et al. (quoted in Ref. 1) agrees also with ours within the experimental errors, whereas a difference of about 56% is verified between the present result and that reported by Arruda-Neto et al.[21]. Finally, for Pb, the cross-section value obtained in the present experiment is 3 or 4 times

greater than other reported data, but in this case the targets differed in their isotopic composition.

3.4. - Nuclear fissility. - The nuclear fissility is the quantity which gives the total fission probability after absorption of a photon by the nucleus, and it is defined as

$$f = \frac{\sigma_f(k)}{\sigma_a^T(k)} \quad , \quad (5)$$

where σ_f is the photofission cross section and σ_a^T is the total nuclear photoabsorption cross section, both quantities being measured at the same photon energy k. In the present work, σ_a^T was evaluated by using Levinger's modified quasi-deuteron model[23] through the expression

$$\sigma_a^T = L \, \frac{NZ}{A} \, \sigma_d(k) \, e^{-D/k} \quad , \quad (6)$$

where σ_d is the total photodisintegration cross section of the free deuteron, NZ is the number of neutron-proton pairs in a nucleus of mass number A, and L and D are, respectively, the so-called "Levinger's" and "damping" parameters. From a very recent analysis by Terranova et al.[32] of total nuclear photoabsorption cross section data in the range 35-140 MeV, the following values for the parameters have been obtained: L = 6.1 and D = 0.72 $A^{0.81}$ MeV. At

photon energy k = 69 MeV, σ_d is 0.108 mb, as it can be deduced from the measurements taken with the LADON photon beams at Frascati by Bernabei et al.[9]. From these data, σ_a^T can be calculated as

$$\sigma_a^T = 0.66Z \left(1 - \frac{Z}{A}\right) e^{-0.0104 \; A^{0.81}} \quad mb, \; k = 69 \; MeV, \qquad (7)$$

and thus the fissilities are obtained from Eq. (5). Values of σ_a^T as well as experimental nuclear fissility at 69 MeV are reported in Table IV for various target nuclei.

4. - Comparison with estimates and discussion.

A simplified description of fission reactions induced by photons of moderate energy like the ones considered in the present work is discussed in this section. To allow a comparison with experimental data, fissility values are calculated from a two-step model in which, during the first, the incident photon is assumed to be absorbed by the target nucleus via the interaction with a neutron-proton pair and, during the second one, the residual nucleus de-excites by a mechanism of competition between fission and particle evaporation processes. The calculation is performed at photon energy of 69 MeV for the nuclei listed in Table IV and, in a systematic way, for those located in the beta-

stability valley, extending from silver up to neptunium. This enabled us to see some interesting structures in the trend of fissility with Z^2/A.

4.1. - A simple model. - The nucleus is assumed to be a degenerate Fermi gas of neutrons and protons confined within a spherically symmetric nuclear potential of radius $R = r_0A^{1/3}$. The primary interaction is considered to take place between the incident photon and a neutron-proton pair (quasi-deuteron), the photon energy being shared by the neutron and proton. Since there are NZ possibilities of forming a n-p pair from nucleons which are moving at random, the kinetic energy gained either by the neutron or proton after the interaction is $\leq$ 50 MeV[33] but, in the average, it is greater than the corresponding Fermi energies for neutrons and protons. In addition, for nuclei of A $\gtrsim$ 100 the proton kinetic energies are always lower than the nuclear cut-off energies for protons (the cut-off energy is calculated as the Fermi energy plus the average binding energy of the loosest nucleon plus, in the case of protons, the Coulomb energy at surface) and, in the cases where this condition is not verified for neutron, its average escape probability during this rapid step of the reaction can be estimated as negligible[34]. This means that simple direct γ-nucleon reactions do not play a significant role at this stage. Therefore, the target nucleus absorbes all the incident photon energy, resulting, after equilibrium, in a nucleus with excitation energy $E^* \approx \overline{k} = 69$ MeV. This result

is also predicted by detailed Monte Carlo calculations of photon-induced intranuclear cascades at this incident energy[24].

Since the energy absorbed is relatively low, the significant de-excitation channels at the second stage of the reaction are neutron emission and fission, and, for intermediate-mass nuclei, proton emission should also be considered. Thus, working in a systematic way, the total level width for the nuclear de-excitation modes is given by $\Gamma_t = \Gamma_n + \Gamma_p + \Gamma_f$ and, in this case, the first-chance fission probability is calculated by

$$P_{f_1} = \frac{\Gamma_f/\Gamma_n}{1 + \Gamma_f/\Gamma_n + \Gamma_p/\Gamma_n} \quad . \tag{8}$$

Of course, P_{f_1} does not represent the nuclear fissility because the subsequent fission chances after successive particle emission are not included yet. However, when $P_{f_1} \approx 1$ (as in the case of nuclei of $A \geq 230$) or $P_{f_1} \ll 1$ (which is verified for nuclei of $A \leq 210$) the fissility is, to a very good approximation, given by the first-chance fission probability, i.e., $f = P_{f_1}$, otherwise $P_{f_1} < f$. But in this latter case, it is expected that P_{f_1} does retain the same trend as fissility.

The ratio Γ_f/Γ_n can be obtained from the statistical

model[35] as

$$\frac{\Gamma_f}{\Gamma_n} = \frac{15a_n^{1/2}(E^*-B_f)^{1/2}}{2r^{1/2}A^{2/3}(E^*-B_n)} \cdot$$

$$\exp\left\{2a_n^{1/2}\left[r^{1/2}(E^*-B_f)^{1/2}-(E^*-B_n)^{1/2}\right]\right\} , \qquad (9)$$

where $r = a_f/a_n$ is the ratio of the level density parameter at the fission saddle point to that of the residual nucleus after neutron evaporation, B_n is the neutron binding energy, B_f is the fission barrier corrected to nuclear temperature, where energies are expressed in MeV. Such a correction has been assumed of the form[36]

$$B_f = B_{f_o}\left(1 - \frac{E^*}{B}\right) , \qquad (10)$$

in which B_{f_o} is the fission barrier at the ground state of the nucleus and B is the nuclear binding energy. In the present calculation, we adopted, for the level spacing parameter a_n, the expression proposed by Iljinov at al.[25], which incorporates corrections due to excitation energy and shell effects as well. Accordingly,

$$a_n = (0.134 \ A - 1.21 \cdot 10^{-4} A^2) \ \cdot$$

$$\cdot \left[1 + \left[1 - \exp(-0.061 \ E^*) \right] \frac{\Delta M}{E^*} \right] \ \text{MeV}^{-1} \quad , \qquad (11)$$

where ΔM is the shell correction to the nuclear mass.

For the ratio Γ_p/Γ_n the following expression deduced from the statistical model by Weisskopf[37] was used:

$$\frac{\Gamma_p}{\Gamma_n} = \frac{E^* - B_p - V_p}{E^* - B_n} \ \cdot$$

$$\exp \left[2a_n^{1/2} \left[(E^* - B_p - V_p)^{1/2} - (E^* - B_n)^{1/2} \right] \right] \quad . \ (12)$$

Here, B_p is the proton binding energy and V_p is the Coulomb barrier for protons at the nuclear surface, corrected to nuclear temperature as it was done in the case of fission barrier (Eq. (10)).

4.2. - Calculated fissility - The calculation was carried out using for ΔM and B_{f_0} the values obtained from the droplet model of the nucleus[38], while for the quantities B, B_n and B_p the values were taken from the 1983 Atomic Mass

Evaluation[39]. Figure 4 illustrates the influence of shell effects on the quantities ΔM, a_n and B_f. This will be reflected in the final values of fissility. For the parameter $r = a_f/a_n$, it is verified that their values are not well defined in the literature, which gives r-values ranging between 1.05 and ~ 1.30 [35]. Since, unfortunately, the results of the calculated fissility are very sensitive to the values of a_f/a_n, we determined a_f/a_n in a semi-empirical way by assuming the simple model described above and by making use of a number of available experimental data on fissility obtained at 36-75 MeV of excitation energy. The data include all those reported in Table IV of the present paper and the ones compiled by Vandenbosch and Huizenga (Table VII- 1 of Ref.35).

These give a total of 30 measured f-values altogether for compound nuclei ranging from Sm up to U. Values of $r = a_f/a_n$ obtained in this way were plotted as function of Z^2/A and, surprisingly, they could be well fitted with straight lines, the equations of which are:

$$r = 1 + 0.05917 \ (Z^2/A - 34.34) \quad , \quad Z^2/A \gtrsim 34.90 \tag{13}$$

$$r = 1 + 0.08334 \ (Z^2/A - 30.30) \quad , \quad 31.20 < Z^2/A \leq 34.00 \tag{14}$$

$$r = 1.281 - 0.01842 \ (Z^2/A - 20.00), \quad 24.90 \leq Z^2/A \leq 31.20 \tag{15}$$

For intermediate-mass nuclei below ^{154}Sm ($Z^2/A \leq 24.90$) it was assumed Eq.(15) to be valid down to Ag ($Z^2/A = 20.45$),

keeping in mind that for this range of nuclei a_f/a_n could not be determined from experiment. In addition, for preactinide nuclei it was not possible to estimate a_f/a_n since fissility data available do not exist. Apart from these restrictions, Eqs. (13-15) can be used to evaluate the ratios a_f/a_n within 1-2 % of uncertainty.

Before entering an extensive calculation of fissility for a number of nuclei, it is worthwhile to discuss some phenomenological aspects of the model itself. First, it was examined for the influence of fast nucleon emission on the calculated fissility. As reported by Leprêtre et al.[11], the emission of both fast neutron and proton during the precompound stage of the decay plays an important role in explaining intermediate-energy ($\sim$ 30-140 MeV) (γ,xn) reactions of complex nuclei. In the case of ^{208}Pb excited by $\sim$ 70-MeV photons, according to Ref.11 the 56% of interactions lead to the emission of a fast neutron taking away a mean total energy of 27 MeV; in the 20 % of the cases a fast proton is emitted, removing out a mean total energy of 38 MeV,whereas in the remaining 24% of the cases no fast particles are emitted.

Taking into account these data we studied the effect of fast nucleon emission on calculated fissility for both actinide and non-actinide nuclei. Calculations have indicated that, for actinides, the fissilities are as much as the same, while for non-actinides the emission of fast

nucleon causes a reduction in fissility of a factor of ~ 4 as compared with that calculated without considering fast nucleon emission. Both results have shown to be independent of a_f/a_n. Since the calculated f-values depend strongly on the parameter a_f/a_n, one may take or not into consideration the emission of fast nucleons in interpreting the photofission data. In the former case and for non-actinide nuclei, a_f/a_n-values are required to be larger of ~ 4.5% with respect to those calculated by disregarding fast nucleon emission. For instance, in the case of ^{208}Pb, one would have 1.228 instead of 1.173 for the a_f/a_n parameter. Since information on fast nucleon emission is available only for a few nuclei, we decided to perform the present calculations without considering such emission throughout. As remarked by Leprêtre et al.[11], it is essential however to consider fast nucleon emission in explaining the decaying of nuclei through intermediate-energy (γ,xn) reactions and photofission reactions as well, in the framework of a more refined model.

The second aspect refers to a possible contribution to calculated fissility from second- and higher-order chance fission probabilities when $P_{f_1} < < 1$. We studied this point to some detail, and the conclusion emerged that second- and higher-order chance fission probabilities do not contribute significantly to calculated fissility. For an initial, compound nucleus in the region Au-Pb-Bi and below, excited to 69 MeV, fissility values calculated by the

approximation $f = P_{f_1}$ have shown to be only ~ 25-30% lower than the correct f-values (i.e. when all subsequent chance fission probabilities are considered). Therefore the expected shell effects in the vicinity of ^{208}Pb will not be significantly weakened by successive neutron evaporation. Such results are illustrated in Fig.5. The approximation $f \simeq P_{f_1}$ is of course no longer valid for pre-actinide nuclei.

Fissility values calculated by the above described method are listed in Table IV (last column). In the case of the ^{nat}Pb target the contribution of naturally occurring Pb isotopes to the calculated fissility has been taken into account. The results of our calculation as a whole fit the available experimental data within a 40% deviation (1σ), or a factor of ~ 2 (2σ). Agreement between estimated and measured fissilities can thus be considered rather satisfactory. Substantial agreement is found for ^{237}Np, ^{232}Th, ^{nat}Pb, ^{208}Pb, ^{197}Au, ^{174}Yb and ^{154}Sm.

Deviations are found, on the contrary, for ^{209}Bi (this work and Ref.20), ^{238}U (this work, Ref.20, Ref. 11) and ^{235}U (this work).

In Fig. 6 fissility values are reported as a function of z^2/A. The experimental results (points) are those from Table IV.

Fissility values calculated (evaporation – fission competition model) for nuclei ranging from silver up to

neptunium along the β-stability valley are connected by a full line. Exceptions are ^{174}Yb and ^{154}Sm nuclei reported for the sake of comparison with experimental data. The dashed lines are drawn in the Z^2/A regions where the ratio a_f/a_n is not experimentally determined. Structures due mainly to shell effects are clearly manifested and put in evidence by the experimental data, specially in the region of lead, as one can appreciate from inspection of the inserted graph in Fig.6.

5. - Conclusion

In the course of the present work, the fission of some actinide nuclei (^{232}Th, ^{238}U and ^{235}U) and some heavy-metal nuclei (^{197}Au, ^{nat}Pb and ^{209}Bi) induced by monochromatic and polarized photons of 69 MeV has been investigated. Absolute photofission cross sections and fissilities were obtained and, in the case of ^{238}U, the influence of photon polarization on fission direction was also studied. The present results did not evidentiate anisotropy in the azimuthal distribution of fission fragment.

Fissility data from the present experiment together with those from other laboratories have been interpreted on the basis of a simple model for photofission reactions, i.e the absorption of the incident photon by neutron-proton pairs inside the nucleus (Levinger's photoabsorption mechanism) followed by a competition between fission and neutron evaporation for the excited compound nucleus.

Fissilities calculated by means of this model show a rather good agreement with the measured ones, and the trend of the fissility vs. Z^2/A obtained for nuclei from silver up to neptunium shows structures, more enhanced in the region $Z = 82$, $N = 126$, which are ascribed to shell effects.

In spite of the limited number of measurements and of the uncertainties associated with both measured and calculated results, we think that the data here presented are sufficient to confirm the predicted shell effects on fission in the vicinity of ^{208}Pb. As conclusion, the present results are very interesting and they should stimulate further experimental and theoretical studies of the photofission reactions in the quasi-deuteron region of photointeraction.

Acknowledgments

FIGURE CAPTIONS

Fig. 1. - Schematic view of the experimental arrangement. The ^{238}U targets have been exposed perpendicularly to incident photon-beam direction.

Fig. 2. - Sample spectra (normalized to one photon) produced by the LADON system obtained by a magnetic pair spectrometer for nominal end-point energy $k_{max}= 78.8$ MeV. Effective photon mean energies, $\bar{k}$, are indicated.

Fig. 3. - Azimuthal angle distribution of ^{238}U fission fragments obtained from incidence of a polarized and monochromatic photon beam of 78.8 MeV maximum energy.

Fig. 4. - Influence of shell effects on the quantities ΔM (experimental mass minus droplet mass, Ref. 38), a_n (level spacing parameter, Eq.(11)) and B_f (fission barrier corrected for nuclear temperature, Eq.(10)) for a nuclear excitation energy of 69 MeV (see text).

Fig. 5. - Calculated first-chance fission probability, $P_{f_{n+1}}$, and total fission probability (fissility, f_n) after evaporation of n neutrons from an initial, compound nucleus excited to 69 MeV. Different symbols refer to different initial nuclei as indicated. Results are normalized at n = 0, and the lines are drawn to guide the eye.

Fig. 6. - Nuclear fissility plotted against parameter Z^2/A for incident photon mean energy (excitation energy) of 69 MeV. Experimental results (points) are those reported in Table IV: ■, ^{237}Np and ^{238}U (Ref. 16); O, ^{235}U, ^{238}U and ^{232}Th (Ref. 11); △, ^{238}U, ^{209}Bi, ^{208}Pb, ^{174}Yb and ^{154}Sm (Ref. 20); □, ^{209}Bi (Ref. 21); ▽, ^{209}Bi (D. TÜRCK et al., quoted in Ref. 1); ◊, ^{208}Pb (Ref. 22); ●, ^{235}U, ^{238}U, ^{232}Th, ^{209}Bi, ^{nat}Pb and ^{197}Au (this work). The full broken line connects estimated fissility values; the dashed lines are used for regions of Z^2/A where the ratio a_f/a_n is not known from experiment (for details, see text). The inserted figure shows the region Ir-Bi where shell effects appear clearly in the vicinity of ^{208}Pb.
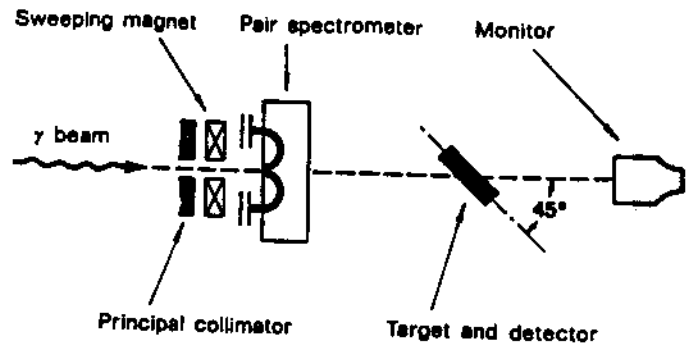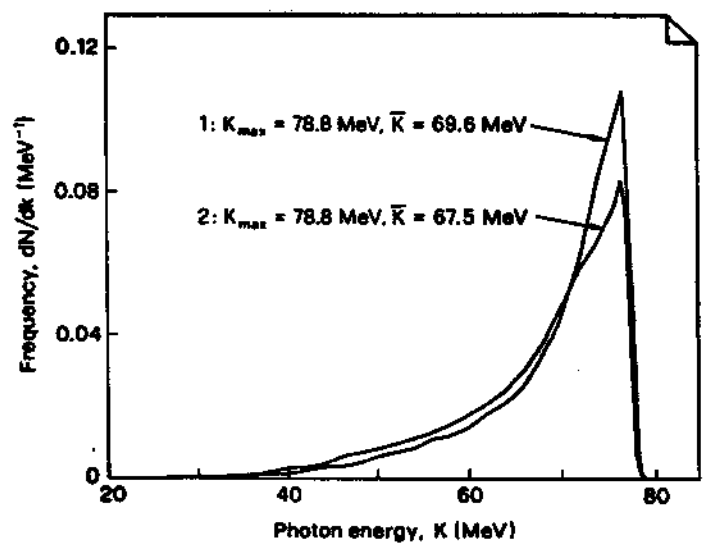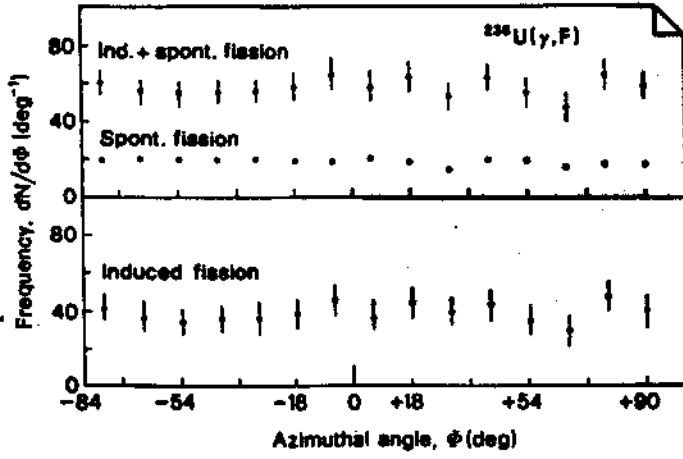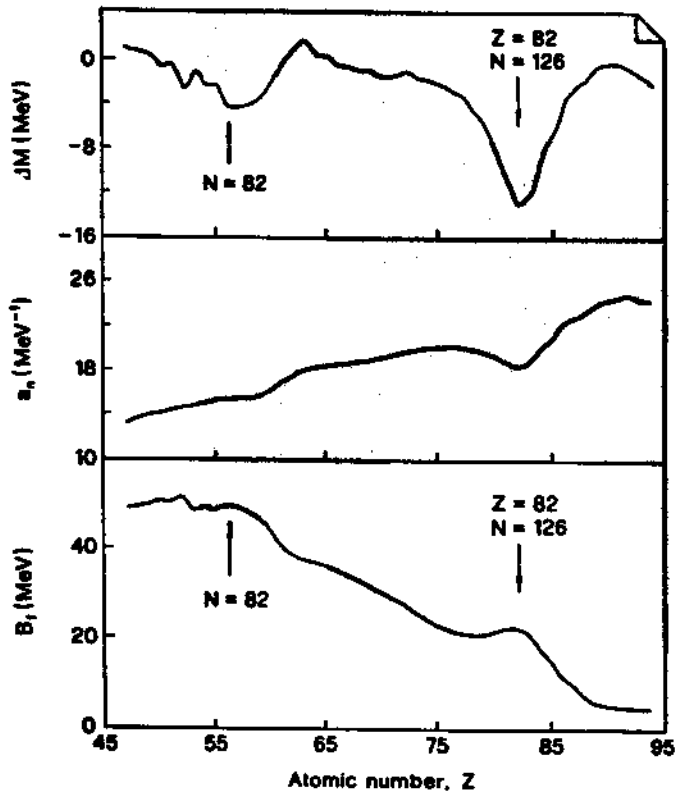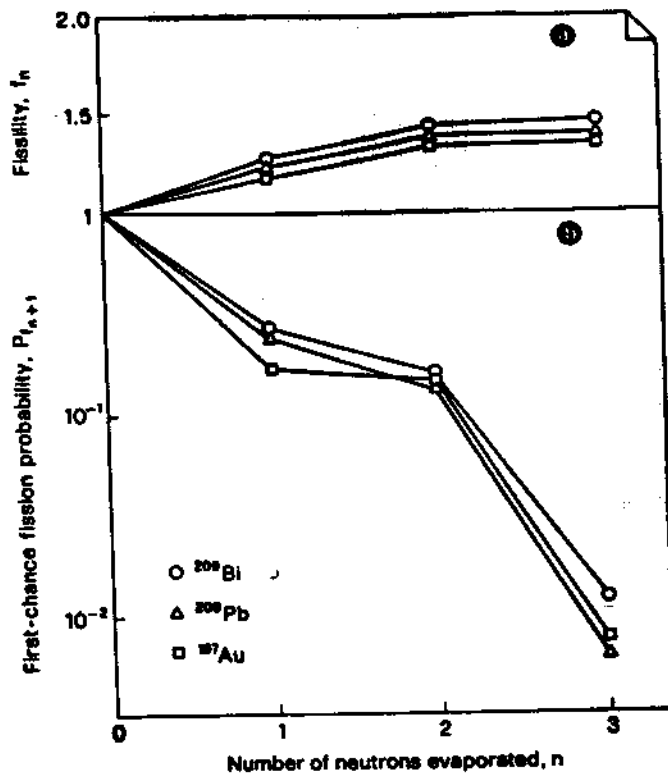
Fig. 1

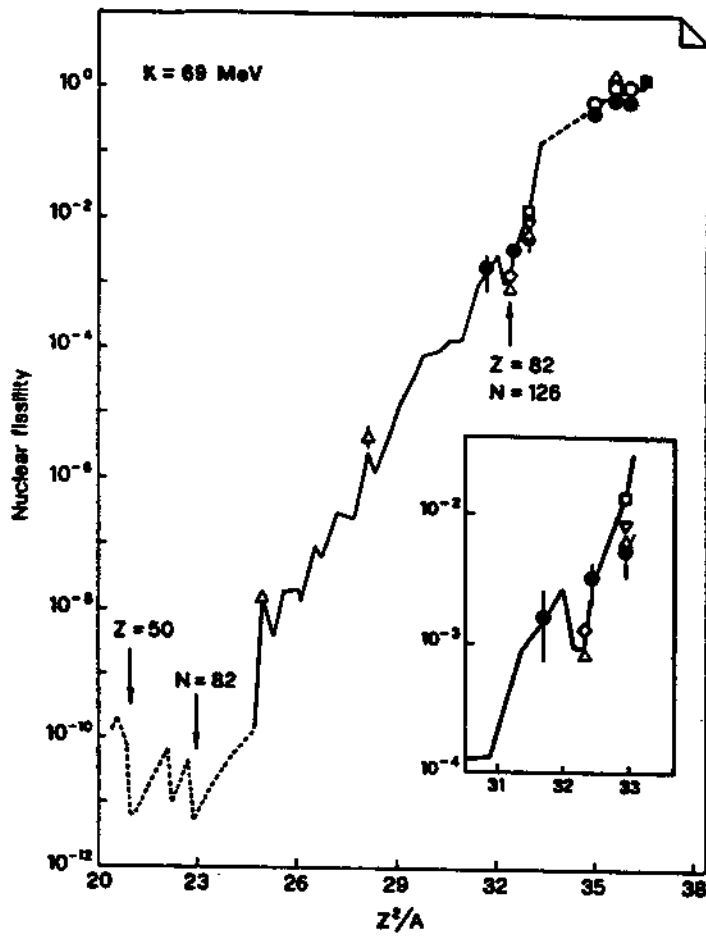Fig. 2

Fig. 3

Fig. 4

Fig. 5

Fig. 6

TABLE I. — *Some data regarding the samples and the exposures to LADON photon beams.*

| Target nucleus | Target-Detector stacks | | | Irradiation conditions[+] | | | |
	Detector	Number of samples	Total thickness (g/cm²)	Effective photon mean energy[‡] $\bar{k}$ (MeV)	Total dose[$] Q($10^9$ γ's)	Beam diameter at the stacks (mm)	Position of the stacks relative to beam direction
^{197}Au	Makrofol	24	0.36	69.6	5.7	9	45°
^{nat}Pb	Makrofol	24	0.43				
^{209}Bi	Makrofol	24	0.47				
^{232}Th	Mica	10	0.33				
^{238}U	Makrofol[*]	15	0.63	67.5	6.9	8	90°
^{232}Th	Mica	10	0.33	68.4	8.0	13	90°
^{235}U	Mica	4	0.19				

[+]Data were taken in three runs.

[*]Better choice to measure azimuthal angle.

[‡]Photon maximum energy of 78.8 MeV in all runs.

[$]Beam intensity of ∼ 10^5 γ/s.

TABLE II. — *Track-etch procedures and microscopy.*

Target and detector	Etching condition	Optics* Objetive	Optics* Ocular	Total area scanned (cm²)	Total of tracks recorded	Mean counting efficiency
Au,Pb,Bi makrofol	6.25-N NaOH,60°C 1h, no stirring	10X,25X	10X	69 (per target)	78 (all targets)	0.78
Th, mica	40% HF, ∼30°C 50min,no stirring	25X,45X	10X	43+ (two runs)	4.0×10^2 (two runs)	0.92
^{238}U makrofol	6.25-N NaOH, 80°C 10min with stirring	10X,45X	10X	60	2.4×10^3	0.95
^{235}U,mica	40% HF, ∼26°C 1 h, no stirring	25X,45X	10X	18	8.4×10^2	0.91

*Leitz Ortholux.
+Not all Th-samples were analysed.

TABLE III. — *Data regarding the determination of the photofission yields.*

Target	Effective number of atoms N_a (10^{18} cm^{-2})(*)	Number of incident photons Q (10^9)	Number of photon-induced fission-tracks N (**)	Fraction of fission events due to low-energy bremsstrahlung γ	Mean total efficiency $\bar\varepsilon$	Photofission yield Y (mb) (***)
Au	$2.0 \cdot 10^2$	5.7	9	-	0.33	$(2.4 \pm 1.4) \cdot 10^{-2}$
Pb	$5.7 \cdot 10^2$		24	-	0.15	$(5 \pm 2) \cdot 10^{-2}$
Bi	$5.4 \cdot 10^2$		40	-	0.16	$(8 \pm 3) \cdot 10^{-2}$
Th	5.0		180	0.097	0.89	6.4 ± 0.7
Th	3.7	8.0	128	0.070	0.89	5 ± 1
^{235}U	1.9		137	0.14	0.89	9 ± 2
^{238}U	8.5	6.9	593	0.095	0.96	10 ± 1

(*) Including all samples analysed.

(**) Corrected for counting loss and geometry.

(***) Statistical plus systematic errors.

TABLE IV. — *Absolute photofission cross section and fissility at 69-MeV photon mean energy.*

Target nucleus	z^2/A	Total nuclear photoabsorption cross section σ_a^T (mb)	Photofission cross section σ_f (mb)	Nuclear fissility experimental	Nuclear fissility calculated
$^{237}_{93}$Np	36.49	15.6	19±4 (*) (a)	1.2±0.3	0.98±0.01
$^{235}_{92}$U	36.02	15.5	15±3 (b) 9±2 (c)	0.97±0.19 0.58±0.13	0.89±0.04
$^{238}_{92}$U	35.56	15.5	15±1 (b) 23±1 (d) 13±2 (*) (a) 10±1 (c)	0.97±0.06 1.48±0.06 0.84±0.13 0.65±0.06	0.83±0.06
$^{232}_{90}$Th	34.91	15.4	9±1 (b) 6±1 (**) (c)	0.58±0.06 0.40±0.06	0.53±0.11
$^{209}_{83}$Bi	32.96	15.0	$(8.0\pm0.6)\cdot10^{-2}$ (d) $(18\pm3)\cdot10^{-2}$ (e) $(12\pm2)\cdot10^{-2}$ (f) $(8\pm3)\cdot10^{-2}$ (c)	$(5.3\pm0.4)\cdot10^{-3}$ $(1.2\pm0.2)\cdot10^{-2}$ $(0.8\pm0.1)\cdot10^{-2}$ $(5\pm2)\cdot10^{-3}$	$(1.3=0.5)\cdot10^{-2}$
$^{nat}_{82}$Pb	32.45	14.9	$(5\pm2)\cdot10^{-2}$ (c)	$(3\pm1)\cdot10^{-3}$	$(2.8=1.0)\cdot10^{-3}$
$^{208}_{82}$Pb	32.33	14.9	$(12\pm2)\cdot10^{-3}$ (d) $(18\pm3)\cdot10^{-3}$ (g)	$(0.8\pm0.1)\cdot10^{-3}$ $(1.2\pm0.2)\cdot10^{-3}$	$(0.9=0.3)\cdot10^{-3}$
$^{197}_{79}$Au	31.68	14.7	$(2.4\pm1.4)\cdot10^{-2}$ (c)	$(1.6\pm0.9)\cdot10^{-3}$	$(1.5\pm0.6)\cdot10^{-3}$
$^{174}_{70}$Yb	28.16	14.0	$(6\pm1)\cdot10^{-5}$ (d)	$(4\pm1)\cdot10^{-6}$	$(2.3=0.9)\cdot10^{-6}$
$^{154}_{62}$Sm	24.96	13.2	$(1.8\pm0.4)\cdot10^{-7}$ (d)	$(1.4\pm0.3)\cdot10^{-8}$	$(1.6=0.5)\cdot10^{-8}$

(*) Interpolated value.

(a) Ref. [16].

(b) Ref. [11].

(c) This work

(d) Ref. [20].

(**) Mean value from two runs.

(e) Ref. [21].

(f) D. TÜRCK *et al.*, quoted in Ref. [1].

(g) Ref. [22].

REFERENCES

[1] H.-D. LEMKE, B. ZIEGLER, M. MUTTERER, J.P. THEOBALD and N. CĂRJAN: Nucl. Phys. A, $\underline{342}$, 37 (1980).

[2] A. LEPRÊTRE, H. BEIL, R. BERGÈRE, P. CARLOS, J. FAGOT, A.DE MINIAC and A. VEYSSIÈRE: Nucl. Phys. A, $\underline{367}$, 237 (1981).

[3] V.G. NEDOREZOV: Proceedings of the Fourth Course of the International School of Intermediate Energy Nuclear Physics , San Miniato (Italy)(1983), p. 434.

[4] M.P. DE PASCALE, G. GIORDANO, G. MATONE, P. PICOZZA, D. BA-BUSCI, R. BERNABEI, L. CASANO, S. D'ANGELO, M. MATTIOLI, D. PROSPERI, C. SCHAERF, S. FRULLANI and B. GIROLAMI: Pro - ceedings of the Fourth Course of the International School of Intermediate Energy Nuclear Physics, San Miniato (Ita - ly)(1983), p. 412.

[5] V. BELLINI: Proceedings of the Fourth Course of the Interna tional School of Intermediate Energy Nuclear Physics, San Miniato (Italy)(1983), p. 251.

[6] H. RIES, U. KNEISSL, G. MANK, H. STRÖHER, W. WILKE, R. BER-GÈRE, P. BOURGEOIS, P. CARLOS, J.L. FALLOU, P. GARGANNE, A. VEYSSIÈRE and L.S. CARDMAN: Phys. Lett. B, $\underline{139}$, 254 (1984).

[7] M.P. DE PASCALE, G. GIORDANO, G. MATONE, D. BABUSCI, R. BER NABEI, O.M. BILANIUK, L. CASANO, S. D'ANGELO, M. MATTIOLI , P. PICOZZA, D. PROSPERI, C. SCHAERF, S. FRULLANI and B. GI-ROLAMI: Phys. Rev. C, $\underline{32}$, 1830 (1985).

[8] N. DE BOTTON: Proceedings of the Fifth Course of the International School of Intermediate Energy Nuclear Physics, Verona (Italy)(1985), p. 114.

[9] R. BERNABEI, A. INCICCHITTI, M. MATTIOLI, P. PICOZZA, D. PROSPERI, L. CASANO, S. D'ANGELO, M.P. DE PASCALE, C.SCHAERF, G. GIORDANO, G. MATONE, S. FRULLANI and B. GIROLAMI: Phys. Rev. Lett., $\underline{57}$, 1542 (1986).

[10] C. GUARALDO, V. LUCHERINI, E. DE SANCTIS, P. LEVI SANDRI, E. POLLI, A.R. REOLON, S. LO NIGRO, S. AIELLO, V. BELLINI, V. EMMA, C. MILONE and G.S.PAPPALARDO: Phys. Rev. C, $\underline{36}$, 1027 (1987).

[11] A. LEPRÊTRE, R. BERGÈRE, P. BOURGEOIS, P. CARLOS, J. FAGOT, J.L. FALLOU, P. GARGANNE, A. VEYSSIÈRE, H. RIES, R. GÖBEL , U. KNEISSL, G. MANK, H. STRÖHER, W. WILKE, D. RYCKBOSCH and J. JURY: Nucl. Phys. A, 472, 533 (1987).

[12] S. LO NIGRO, S. AIELLO, G. LANZANÒ, C. MILONE, A. PAGANO , A. PALMERI, G.S. PAPPALARDO, V. LUCHERINI, N. BIANCHI, E. DE SANCTIS, C. GUARALDO, P. LEVI SANDRI, V. MUCCIFORA, E. POLLI, A.R. REOLON and P. ROSSI: Nuovo Cimento A, 98, 643 (1987).

[13] R. BERNABEI, V.C. DE OLIVEIRA, J.B. MARTINS, O.A.P.TAVARES, J.D. PINHEIRO FILHO, S. D'ANGELO, M.P. DE PASCALE, C.SCHAERF, and B. GIROLAMI: Nuovo Cimento A, 100, 131 (1988).

[14] J.B. MARTINS, E.L. MOREIRA, O.A.P. TAVARES, J.L. VIEIRA, J. D. PINHEIRO FILHO, R. BERNABEI, S. D'ANGELO, M.P. DE PASCA-LE, C. SCHAERF and B. GIROLAMI: Nuovo Cimento A, 101, 789 (1989).

[15] V. LUCHERINI, C. GUARALDO, E. DE SANCTIS, P. LEVI SANDRI, E. POLLI, A.R. REOLON, A.S. ILJINOV, S. LO NIGRO, S. AIELLO , V. BELLINI, V. EMMA, C. MILONE, G.S. PAPPALARDO and M.V. MEBEL: Phys. Rev. C, 39, 911 (1989).

[16] D.I. IVANOV, G. YA. KEZERASHVILI, V.V. MURATOV, V.G. NEDORE ZOV, A.S. SUDOV and V.A. ZAPEVALOV: International Conferen-ce, Fiftieth Anniversary of Nuclear Fission,Leningrad(1989).

[17] A.S. ILJINOV, M.V. MEBEL, C. GUARALDO, V. LUCHERINI, E. DE SANCTIS, N. BIANCHI, P. LEVI SANDRI, V. MUCCIFORA, E. POLLI, A.R. REOLON, P. ROSSI and S. LO NIGRO: Phys. Rev. C, 39 , 1420 (1989).

[18] C. GUARALDO, V. LUCHERINI, E. DE SANCTIS, A.S. ILJINOV, M. V. MEBEL and S. LO NIGRO: Nuovo Cimento A, 103, 607 (1990).

[19] P.P. DELSANTO, A. FUBINI, F. MURGIA and P. QUARATI: Pre - print INFN-CA, Cagliari (March, 1990).

[20] L.G. MORETTO, R.C. GATTI, S.G. THOMPSON, J.T. ROUTTI, J.H. HEISENBERG, L.M. MIDDLEMAN, M.R. YEARIAN and R. HOFSTADTER: Phys. Rev., 179, 1176 (1969).

[21] J.D.T. ARRUDA-NETO, M. SUGAWARA, T. TAMAE, O. SASAKI, H. OGINO, H. MIYASE and K. ABE: Phys. Rev. C,34, 935 (1986).

[22] J.D.T. ARRUDA-NETO, M. SUGAWARA, H. MIYASE, T. KOBAYASHI, T. TAMAE, K. ABE, M. NOMURA, H. MATUSUYAMA, H. KAWAHARA , K. NAMAI, M.L. YONEAMA and S. SIMIONATTO: Phys. Rev. C, 41, 354 (1990).

[23] J.S. LEVINGER: Phys. Rev. Lett. B, 82, 181 (1979).

[24] V.S. BARASHENKOV, F.G. GEREGHI, A.S. ILJINOV, G.G. JONSSON and V.D. TONEEV: Nucl. Phys. A, 231, 462 (1974).

[25] A.S. ILJINOV, E.A. CHEREPANOV and S.E. CHIGRINOV: Yad.Fiz., 32, 322 (1980) [Sov. J. Nucl. Phys., 32, 166 (1980)].

[26] H. YAGODA: Radioactive Measurements with Nuclear Emulsions (John Wiley, New York, 1949), p. 53.

[27] L. FEDERICI, G. GIORDANO, G. MATONE, G. PASQUARIELLO, P. PICOZZA, R. CALOI, L. CASANO, M.P. DE PASCALE, M. MATTIOLI, E. POLDI, C. SCHAERF, M. VANNI, P. PELFER, D. PROSPERI, S. FRULLANI and B. GIROLAMI: Nuovo Cimento B, 59, 247 (1980).

[28] M.P. DE PASCALE, G. GIORDANO, G. MATONE, P. PICOZZA, R. CA LOI, L. CASANO, M. MATTIOLI, E. POLDI, D. PROSPERI and C. SCHAERF: Appl. Opt., 21, 2660 (1982).

[29] A.M. SANDORFI, M.J. LEVINE, C.E. THORN, G. GIORDANO, G. MA TONE and C. SCHAERF: IEEE Trans. on Nucl. Sci., NS-30,3083 (1983).

[30] S.N. SOKOLOV and K.D. TOLSTOV: Proceedings of the IV Inter nationalen Kolloquium über Korpuskularphotographie, München (1962), p. 468.

[31] O.A.P. TAVARES: Pre-print CBPF-NF-015/90, Centro Brasilei ro de Pesquisas Físicas, Rio de Janeiro-RJ, (May, 1990).

[32] M.L. TERRANOVA, D.A. DE LIMA and J.D. PINHEIRO FILHO: Euro phys. Lett., 9, 523 (1989).

[33] V. DI NAPOLI, M.L. TERRANOVA, J.B. MARTINS, J.D. PINHEIRO FILHO and O.A.P. TAVARES: Lett. Nuovo Cimento, 23, 424 (1978).

[34] H.G. DE CARVALHO, J.B. MARTINS, O.A.P. TAVARES, R.A.M.S.NA
ZARETH and V. DI NAPOLI: Lett. Nuovo Cimento, 2,1139(1971).

[35] R.VANDENBOSCH and J.R. HUIZENGA: Nuclear Fission (Academic
Press, New York, 1973), Chapter VII.

[36] Y. FUJIMOTO and Y. YAMAGUCHI: Progr. Theor. Phys., 5, 76
(1950).

[37] V.F. WEISSKOPF: Phys. Rev., 52, 295 (1937).

[38] W.D. MYERS: Droplet Model of Atomic Nuclei (Plenum, New
York, 1977).

[39] A.H. WAPSTRA and G. AUDI: Nucl. Phys. A, 432, 1 (1985).